J Wood Sci (1999) 45:275–283


ORIGINAL ARTICLE

**Kosei Ando · Masamitsu Ohta**

# Variability of fracture toughness by the crack tip position in an annual ring of coniferous wood

Received: July 8, 1998 / Accepted: December 11, 1998

**Abstract** The effects of the location of the crack tip in an annual ring and the direction of crack propagation on the fracture toughness of the TR crack propagation system of coniferous wood (T, direction normal to the notch plane; R, propagation direction) were analyzed by the finite element method in regard of the changes in elastic modulus and strength within an annual ring. The critical point of the fracture was defined as the state where the stress of a square element ($0.125 \times 0.125$ mm) in contact with the crack tip equals the tensile strength. The distribution of specific gravity was measured by soft X-ray densitometry. The elastic moduli in the T and R directions were estimated by the sound velocity. The tensile strengths in the T and R directions were measured by the tensile test using small specimens of 1 mm span length. Regarding the variability of fracture toughness ($K_{IC}$), the experimental and calculated results had the same tendency. Therefore, it was concluded that the variability of $K_{IC}$ is caused by the (1) heterogeneity of the elastic modulus and strength within an annual ring; and (2) changes in the degree of stress concentration at the crack tips, according to the direction of crack propagation.

K. Ando (✉)
School of Agricultural Sciences, Nagoya University, Chikusa-ku, Nagoya 464-8601, Japan
Tel. +81-52-789-4149; Fax +81-52-789-4147
e-mail: musica@agr.nagoya-u.ac.jp

M. Ohta
Graduate School of Agricultural and Life Sciences, The University of Tokyo, Bunkyo-ku, Tokyo 113-8657, Japan

Part of this work was presented at the 40th annual meeting of the Japan Wood Research Society, Tsukuba, April 1990 and at the 6th International Conference on Mechanical Behavior of Materials, Kyoto, July 1991

**Key words** Finite element method · Fracture toughness · Annual ring · Porous structure

## Introduction

In previous reports[1,2] the variability of fracture toughness ($K_{IC}$) in an annual ring was measured in the TR crack propagation system (when T refers to the direction normal to the notch plane and R to the propagation direction) of sugi (*Cryptomeria japonica*) and spruce (*Picea sitchensis*). As a result, the critical stress intensity factors ($K_{IC}$), which were calculated from the load at the initiation of a crack, varied according to the location of the crack tip in a single annual ring and the direction of crack propagation (i.e., from pith to bark or from bark to pith). When the crack tip was located in earlywood, the $K_{IC}$ value increased with the decrease in distance between the crack tip and the annual ring boundary in front of it; and when the crack tip was located in latewood, the $K_{IC}$ was relatively small. It is believed that the variability of $K_{IC}$ by the crack tip position in an annual ring is due to: (1) the difference in cell shape or cell-wall thickness around the crack tip; and (2) the difference in stress concentration caused by the location of the crack tip and the direction of crack propagation.

The finite element method (FEM) is useful for calculating stress distributions near the crack tip. In the field of fracture mechanics of wood science, many finite element analyses have been carried out, and studies on crack initiation or the propagation mechanism have been reported.[3-8] However, there is little research that takes into consideration the heterogeneity of wood (e.g., unevenness of mechanical properties in an annual ring) except studies on the stress distribution in cell-wall substances[9,10] or around the knots.[4,7,8]

In this report, the variations of $K_{IC}$ according to the location of the crack tip in an annual ring and the direction of crack propagation were calculated by the FEM, taking into account the heterogeneity of cell properties.

The findings were then compared with the results of experiments.

## Materials and methods

### Specimens

Spruce (*Picea sitchensis* Carr.), sugi (*Cryptomeria japonica* D. Don), and akamatsu (*Pinus densiflora* Sieb. et Zucc.) were used in the experiments and the FEM calculations. Specific gravity, moisture content, and annual ring width of the specimens are shown in Table 1. The single-edge notched-type tensile specimen of the TR crack propagation system was employed. Specimens were designed so all notch tips exist in the same annual ring. Figure 1 illustrates the shapes and sizes of two kinds of specimen: pith-side notched type and bark-side notched type. The specimen width was 25 mm, its thickness 10 mm, and the notch length 11 mm. Using a thin circular saw, the notch was made initially to 10 mm depth and was then extended 1 mm more by a razor blade. The position of the notch tip in the annual ring was determined by microscopy just before the fracture test.

### Fracture toughness test

The fracture toughness tests were performed at 20°C, 65% relative humidity using an electrohydro servo testing machine (Servopulser EHF-EA5; Shimadzu, Kyoto, Japan). Specimens were held by a pin-loading system. The crosshead speed was 1 mm/min. The crack opening displacement (COD) was measured using a clip gauge.

The fracture toughness, ($K_{IC}$), was calculated by the following isotropic equation.[11]

$$K_{IC} = \sigma_C \sqrt{\pi a} F(a/W), \tag{1}$$

$$F(a/W) = 1.12 - 0.231(a/W) + 10.55(a/W)^2 - 21.72(a/W)^3 + 30.39(a/W)^4 \tag{2}$$

where $\sigma_C$ is the nominal critical stress, $a$ is the notch length, $W$ is the specimen width, and $F(a/W)$ is a shape factor. In the present work, the proportional-limit stress was $\sigma_C$, because we recognized visually that the load of crack initiation agreed with the proportional-limit load in the load-COD diagrams.

### Distribution of specific gravity and mechanical properties in a single annual ring

The distribution of specific gravity in an annual ring was measured with soft X-ray densitometry. Softex Type K and Joyce Loebl Microdensitometer 3CS were used as the soft X-ray irradiating device and densitometer, respectively. The results are shown in Fig. 2. The unit of the horizontal axis is defined as shown in Fig. 3.

**Table 1.** Specific gravity, moisture content, and investigated annual ring width

| Species | Specific gravity | Moisture content (%) | Annual ring width (mm) |
|---|---|---|---|
| Sugi (*Cryptomeria japonica* D. Don) | 0.36 (0.00) | 12.4 (0.1) | 5.0 (0.3) |
| Spruce (*Picea sitchensis* Carr.) | 0.44 (0.00) | 12.1 (0.1) | 4.1 (0.2) |
| Akamatsu (*Pinus densiflora* Sieb. et Zucc.) | 0.55 (0.00) | 12.5 (0.0) | 4.8 (0.3) |

Numbers in parentheses are standard deviations

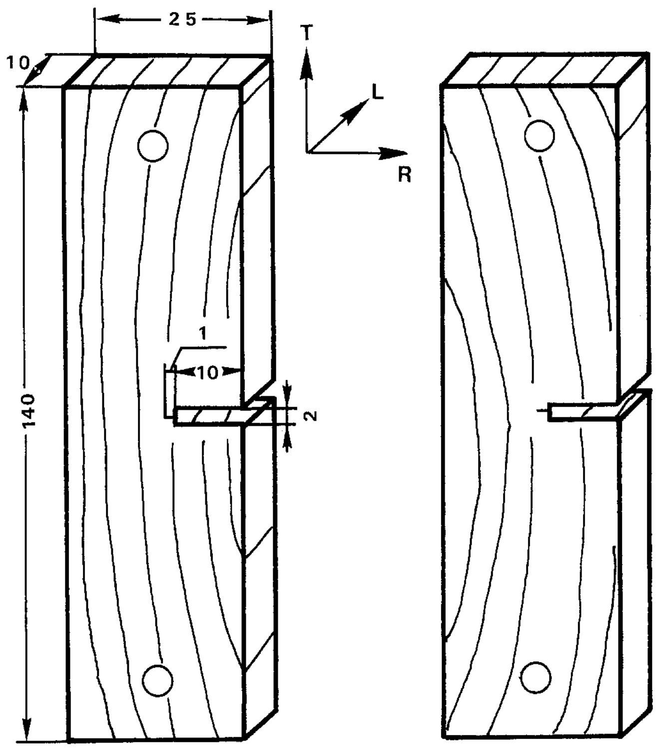


**Fig. 1.** Test specimens. **Left** Pith-side notched. **Right** Bark-side notched. Units are millimeters

The ultrasonic pulse velocity propagating in the material was measured, and the distributions of elastic moduli in a tangential direction ($E_T$) and a radial direction ($E_R$) within an annual ring were estimated by Eq. (3).[12]

$$E = \varrho v^2 \tag{3}$$

where $v$ is the sound velocity; $E$ is the elastic modulus; and $\varrho$ is the density. The specimen sizes were 1 (T) × 1 (R) × 10 (L) mm [for the measurement of $E_T$ (T-specimen)] and 1 (R) × 5 (T) × 5 (L) mm (for the measurement of $E_R$ (R-specimen)]. Both the T and R specimens were continuously obtained from the same single annual ring, which was investigated by the fracture toughness test. A supersonic detector (Ultrasound Tester SM95; Tokyo Keiki, Tokyo, Japan) was used for measuring the sound velocity. The diameter of the transducer was 14 mm. Figure 4 shows the relations between specific gravity and the elastic moduli ($E_T$ and $E_R$)

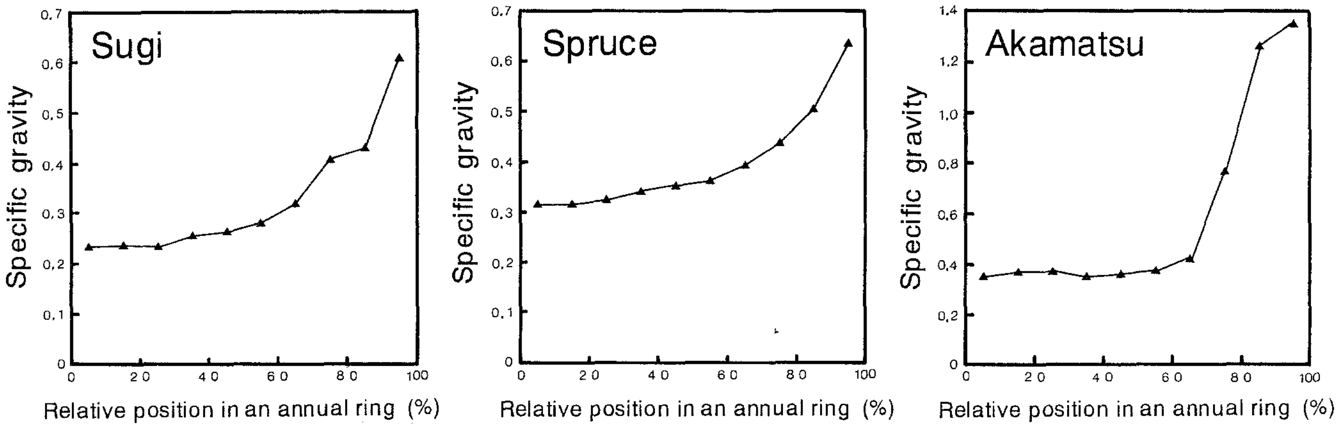


**Fig. 2.** Distributions of the specific gravity in a single annual ring

**Fig. 3.** Definition of the relative position of the crack tip in an annual ring in this study. *A*, annual-ring width; *B*, radial distance from the ring boundary of the previous year

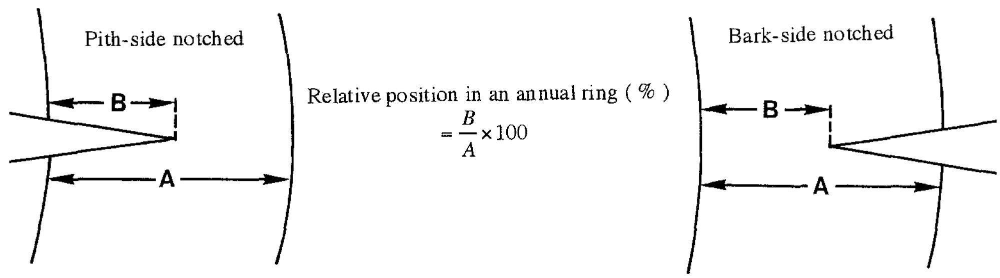


obtained by the sound velocity method. Because the elastic modulus of wood is generally expressed as the exponential power of specific gravity,[13] the distributions of $E_T$ and $E_R$ in an annual ring were obtained using the results of Fig. 2 and the regression equations shown in Fig. 4. The results are shown in Fig. 5.

The distribution of elastic modulus in a longitudinal direction ($E_L$) within an annual ring was measured by the oscillating lead method. The specimens were 0.2 (R) $\times$ 10 (T) $\times$ 50 (L) mm.

The distribution of tensile strength in a tangential direction ($\sigma_{tT}$) and a radial direction ($\sigma_{tR}$) within an annual ring were obtained from the results of an actual tensile test. The specimens were the same as those used for measuring sound velocity. Reinforcing metal plates were bonded as the gripping parts of the specimens. The tensile testing was carried out at a crosshead speed of 0.5 mm/min. Figure 6 shows the relations between the specific gravity and tensile strength ($\sigma_{tT}$ and $\sigma_{tR}$) of sugi, spruce, and akamatsu. The strength of wood is also expressed in the exponential power of the specific gravity.[14] The distributions of $\sigma_{tT}$ and $\sigma_{tR}$ in an annual ring are shown in Fig. 7 using the results of Fig. 2 and the regression equations shown in Fig. 6.

## FEM calculation of fracture toughness

The FEM was applied to analyze how the fracture toughness is affected by the difference in stress distribution that results from the location of the crack tip in a single annual ring and the direction of crack propagation. The program used was a universal FEM program (HITAC ISAS II), which is a library program of the Computer Center of the University of Tokyo. The analyses were carried out with a super computer (HITAC S-820).

Figure 8 shows the finite element meshes used for the numerical calculations. The shaded portion in Fig. 8 corresponds to the analyzed finite element meshes. There were 4534 elements and 4483 grids. The smallest elements (i.e., the elements near the crack tip) are 0.125 $\times$ 0.125 mm squares. The displacement of segment AB in Fig. 8 was fixed in the T direction, and forced displacement was provided to the line DE in Fig. 8 in the T direction, realizing the condition of crack opening.

The annual ring width was 5 mm, divided into 10 sections with different properties (elastic modulus and shearing elastic modulus) from each other. By shifting the property groups in the R direction step by step, we attempted to reproduce the differences in the location of the crack tips within an annual ring. The effect of the curvature of the annual ring was not considered in these FEM meshes. The elastic modulus ($E_T$ and $E_R$) and tensile strength ($\sigma_{tT}$ and $\sigma_{tR}$) of each section in an annual ring were obtained from the above-mentioned procedures. The shearing elastic modulus ($G_{TR}$) was derived from Eq. (4).[15]

$$G_{TR} = 0.003E_L \tag{4}$$

It is assumed that Poisson's ratios ($\nu_{RT}$, $\nu_{LT}$, and $\nu_{LR}$) are constant, and the values noted by Fushitani et al.[13] were used.

**Fig. 4.** Relations between modulus of elasticity and specific gravity

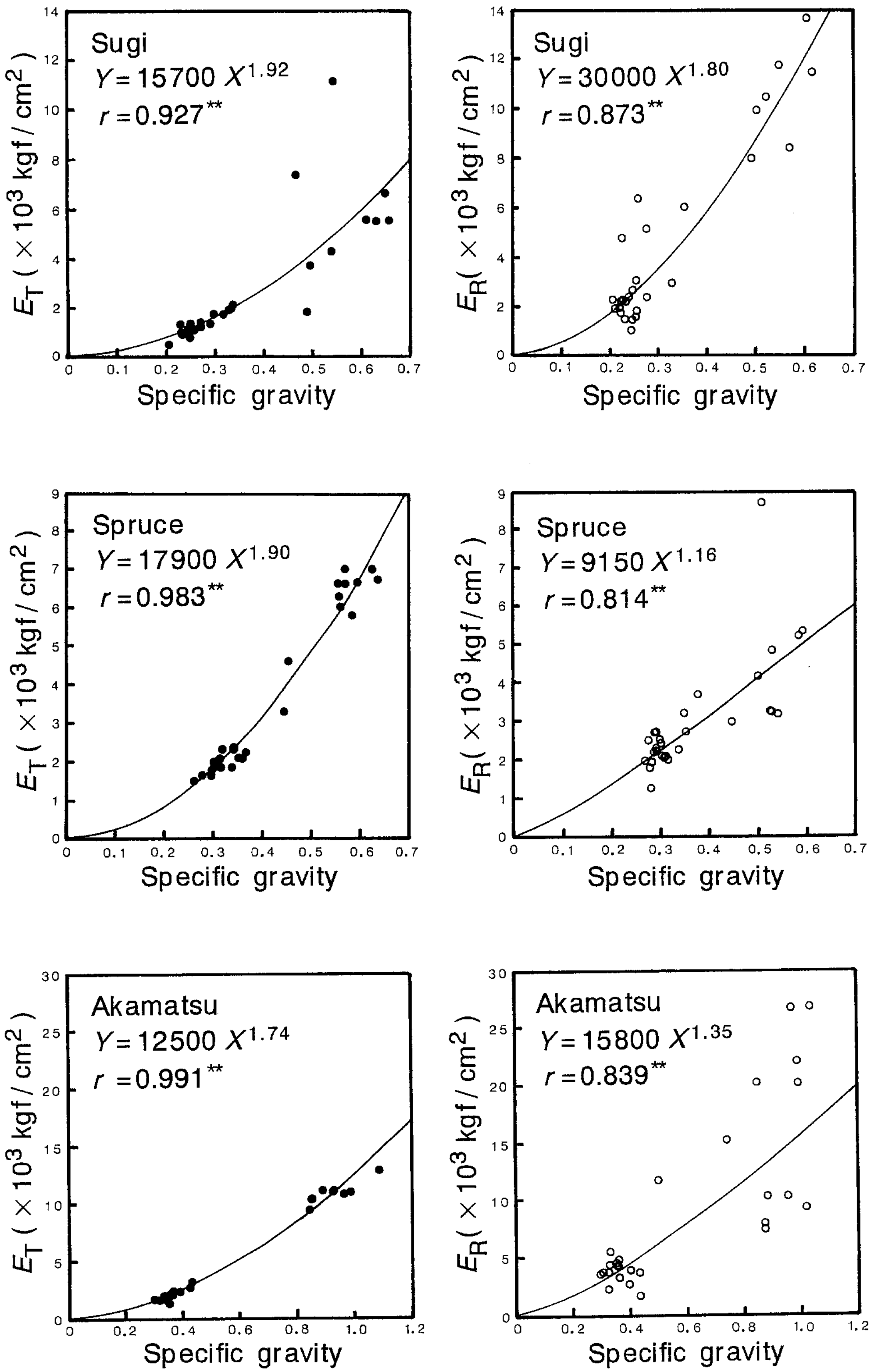

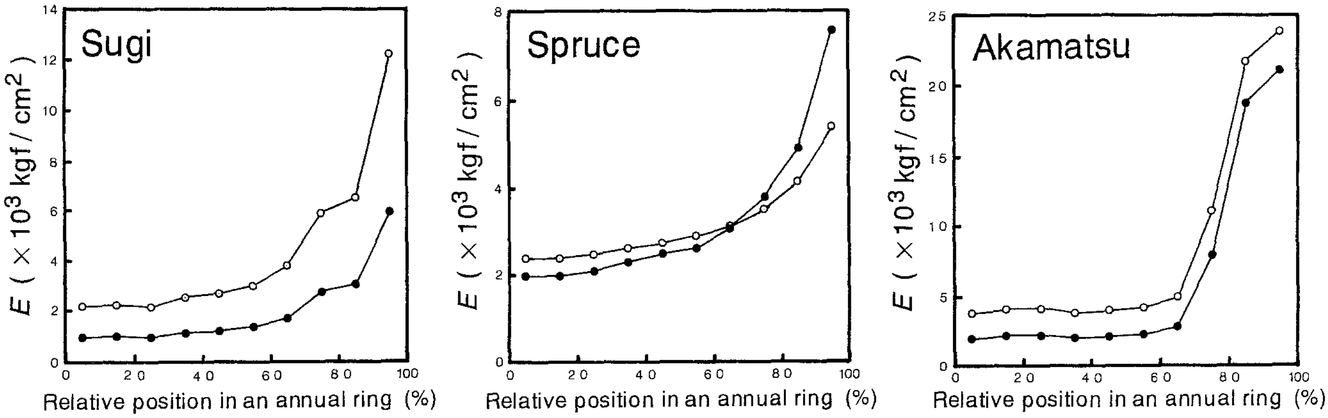


**Fig. 5.** Distributions of the predicted modulus of elasticity in a single annual ring. *Filled circles*, $E_T$; *open circles*, $E_R$

**Table 2.** Mechanical properties in a single annual ring used for finite element method analysis of sugi wood

| Relative position in an annual ring (%) | ($\times 10^3$ kgf/cm$^2$) | | | | (kgf/cm$^2$) | |
|---|---|---|---|---|---|---|
| | $E_T$ | $E_R$ | $E_L$ | $G_{TR}$ | $\sigma_{tT}$ | $\sigma_{tR}$ |
| 0–10 | 0.966 | 2.20 | 53.1 | 0.159 | 23.5 | 32.2 |
| 10–20 | 0.982 | 2.23 | 53.6 | 0.161 | 23.8 | 32.5 |
| 20–30 | 0.958 | 2.18 | 52.9 | 0.159 | 23.3 | 32.0 |
| 30–40 | 1.13 | 2.55 | 57.7 | 0.173 | 27.1 | 35.2 |
| 40–50 | 1.20 | 2.69 | 59.5 | 0.179 | 28.6 | 36.4 |
| 50–60 | 1.36 | 3.03 | 63.6 | 0.191 | 32.1 | 39.2 |
| 60–70 | 1.74 | 3.81 | 72.2 | 0.217 | 40.1 | 45.1 |
| 70–80 | 2.78 | 5.92 | 92.2 | 0.277 | 61.5 | 59.0 |
| 80–90 | 3.09 | 6.54 | 97.4 | 0.292 | 67.8 | 62.7 |
| 90–100 | 6.02 | 12.2 | 138 | 0.414 | 124 | 91.8 |

$E_T$, $E_R$, $E_L$, modulus of elasticity in tangential, radial, and longitudinal directions; $G_{TR}$, modulus of shearing elasticity; $\sigma_{tT}$, $\sigma_{tR}$, tensile strength in tangential and radial directions; $\nu_{LR}$, $\nu_{LT}$, $\nu_{RT}$, Poisson's ratio
$\nu_{LR}$, 0.40; $\nu_{LT}$, 0.60; $\nu_{RT}$, 0.90

**Table 4.** Mechanical properties in a single annual ring used for finite element method analysis of akamatsu wood

| Relative position in an annual ring (%) | ($\times 10^3$ kgf/cm$^2$) | | | | (kgf/cm$^2$) | |
|---|---|---|---|---|---|---|
| | $E_T$ | $E_R$ | $E_L$ | $G_{TR}$ | $\sigma_{tT}$ | $\sigma_{tR}$ |
| 0–10 | 2.04 | 3.85 | 74.6 | 0.224 | 48.1 | 56.8 |
| 10–20 | 2.23 | 4.12 | 78.6 | 0.236 | 51.1 | 60.4 |
| 20–30 | 2.26 | 4.16 | 79.5 | 0.239 | 51.6 | 60.9 |
| 30–40 | 2.05 | 3.86 | 74.8 | 0.224 | 48.3 | 57.0 |
| 40–50 | 2.15 | 4.01 | 77.2 | 0.232 | 50.0 | 59.0 |
| 50–60 | 2.30 | 4.22 | 80.5 | 0.241 | 52.3 | 61.7 |
| 60–70 | 2.82 | 4.95 | 91.6 | 0.275 | 60.4 | 71.2 |
| 70–80 | 7.95 | 11.1 | 177 | 0.530 | 125 | 147 |
| 80–90 | 18.7 | 21.7 | 304 | 0.911 | 228 | 266 |
| 90–100 | 21.0 | 23.7 | 327 | 0.98 | 248 | 288 |

$E_T$, $E_R$, $E_L$, modulus of elasticity in tangential, radial, and longitudinal directions; $G_{TR}$, modulus of shearing elasticity; $\sigma_{tT}$, $\sigma_{tR}$, tensile strength in tangential and radial directions; $\nu_{LR}$, $\nu_{LT}$, $\nu_{RT}$, Poisson's ratio
$\nu_{LR}$, 0.40; $\nu_{LT}$, 0.60; $\nu_{RT}$, 0.65

**Table 3.** Mechanical properties in a single annual ring used for finite element method analysis of spruce wood

| Relative position in an annual ring (%) | ($\times 10^3$ kgf/cm$^2$) | | | | (kgf/cm$^2$) | |
|---|---|---|---|---|---|---|
| | $E_T$ | $E_R$ | $E_L$ | $G_{TR}$ | $\sigma_{tT}$ | $\sigma_{tR}$ |
| 0–10 | 2.00 | 2.38 | 67.2 | 0.202 | 52.0 | 59.5 |
| 10–20 | 2.00 | 2.38 | 67.2 | 0.202 | 52.0 | 59.5 |
| 20–30 | 2.10 | 2.46 | 69.4 | 0.208 | 53.9 | 61.2 |
| 30–40 | 2.31 | 2.60 | 73.3 | 0.220 | 57.2 | 64.4 |
| 40–50 | 2.48 | 2.72 | 76.5 | 0.229 | 59.9 | 67.0 |
| 50–60 | 2.61 | 2.81 | 78.9 | 0.237 | 62.0 | 69.0 |
| 60–70 | 3.07 | 3.10 | 86.8 | 0.260 | 68.9 | 75.4 |
| 70–80 | 3.75 | 3.51 | 97.8 | 0.293 | 78.5 | 84.3 |
| 80–90 | 4.89 | 4.13 | 115 | 0.344 | 93.4 | 97.6 |
| 90–100 | 7.55 | 5.39 | 148 | 0.445 | 124 | 124 |

$E_T$, $E_R$, $E_L$, modulus of elasticity in tangential, radial, and longitudinal directions; $G_{TR}$, modulus of shearing elasticity; $\sigma_{tT}$, $\sigma_{tR}$, tensile strength in tangential and radial directions; $\nu_{LR}$, $\nu_{LT}$, $\nu_{RT}$, Poisson's ratio
$\nu_{LR}$, 0.37; $\nu_{LT}$, 0.47; $\nu_{RT}$, 0.44

The critical point of fracture was assumed to be the load where the stress of one element in contact with the crack tip (Fig. 8B) equaled the tensile strength. The $K_{IC}$ values were calculated by Eq. (1) using nominal stress.

The mechanical properties in a single annual ring for FEM analyses of sugi, spruce, and akamatsu are shown in Tables 2, 3, and 4, respectively.

## Results and discussion

Figure 9 shows the relations between the location of the crack tip in an annual ring and the fracture toughness ($K_{IC}$) values for sugi, spruce, and akamatsu. Experimental values of $K_{IC}$ in Fig. 9 are the same as those in previous reports for sugi[1] and spruce.[2] The results for akamatsu are newly obtained here. The variability of $K_{IC}$ values in an annual ring

**Fig. 6.** Relations between tensile strength and specific gravity

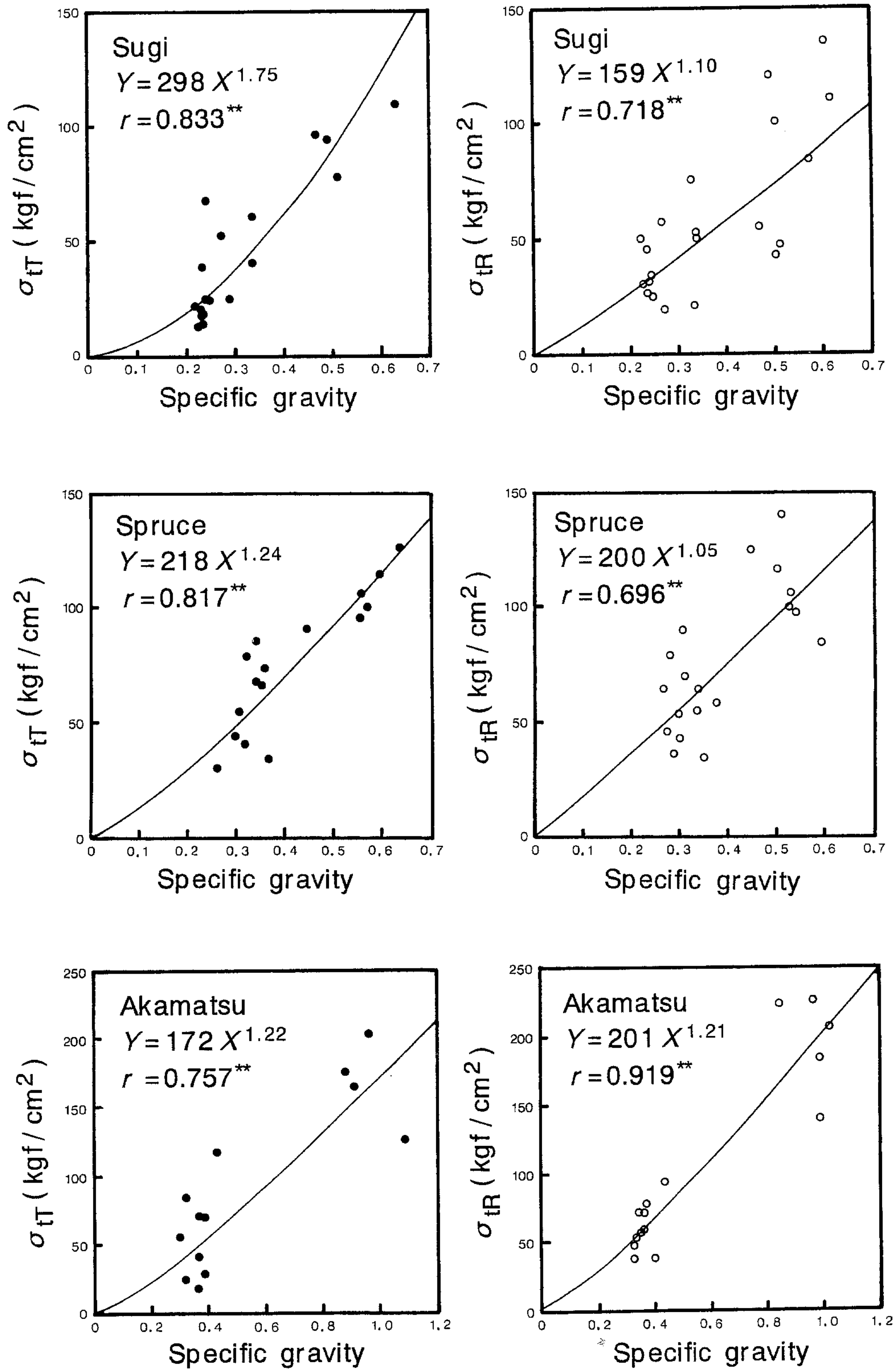

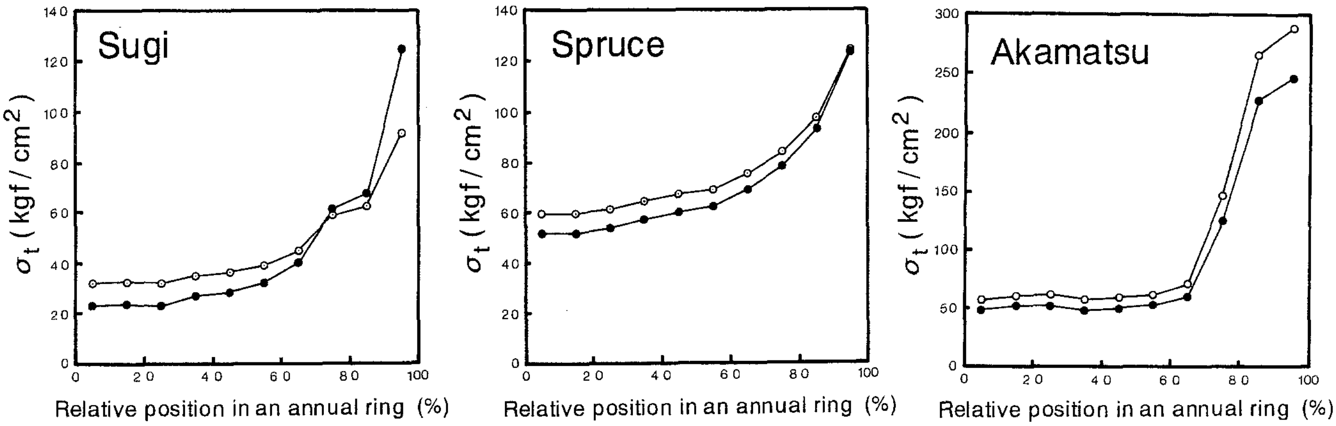


**Fig. 7.** Distributions of the predicted tensile strength in a single annual ring. *Filled circles*, $\sigma_{tT}$; *open circles*, $\sigma_{tR}$

**Fig. 8.** Finite element meshes for the single-edge notched type tensile specimen of TR crack propagation system. Units are millimeters

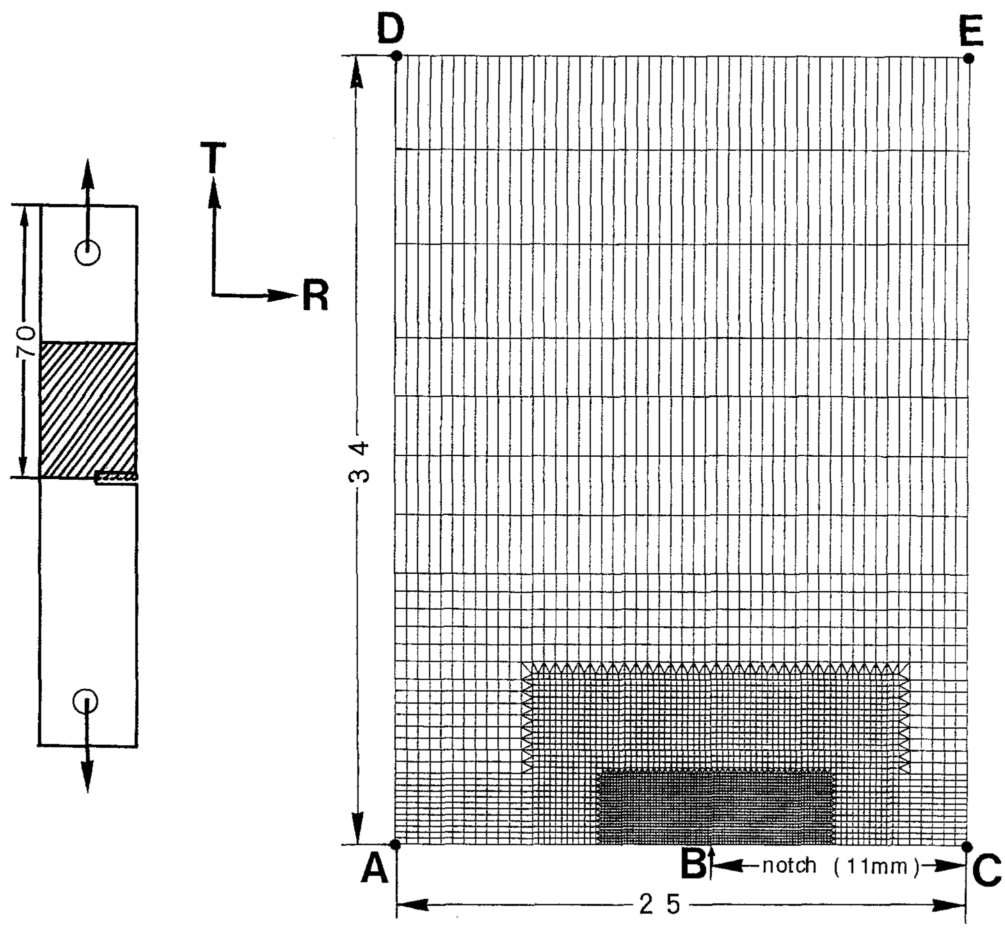


was reconfirmed. The FEM analysis results, shown by the solid line in Fig. 9, were found to be in good agreement with the experimental findings.

For understanding these $K_{IC}$ variations in an annual ring according to the location of the crack tip and the direction of crack propagation, we examined stress concentration around the crack tip. The stress at the tip is expressed by the following equation:

$$\sigma_{tip} = \alpha\sigma \tag{5}$$

where the $\sigma_{tip}$ is a stress at the crack tip in a tangential direction obtained by FEM analysis, $\sigma$ is the nominal stress, and $\alpha$ is the stress concentration factor. The results, shown in Fig. 10, indicate that $\alpha$ differs depending on the propagation direction of the crack (pith-side notched, bark-side notched), even at the same location in an annual ring. The value of $\alpha$ increases with an increase in the relative position in an annual ring. The variability of $K_{IC}$ values derives from this tendency of $\alpha$ and the variation of tensile strength shown in Fig. 7.

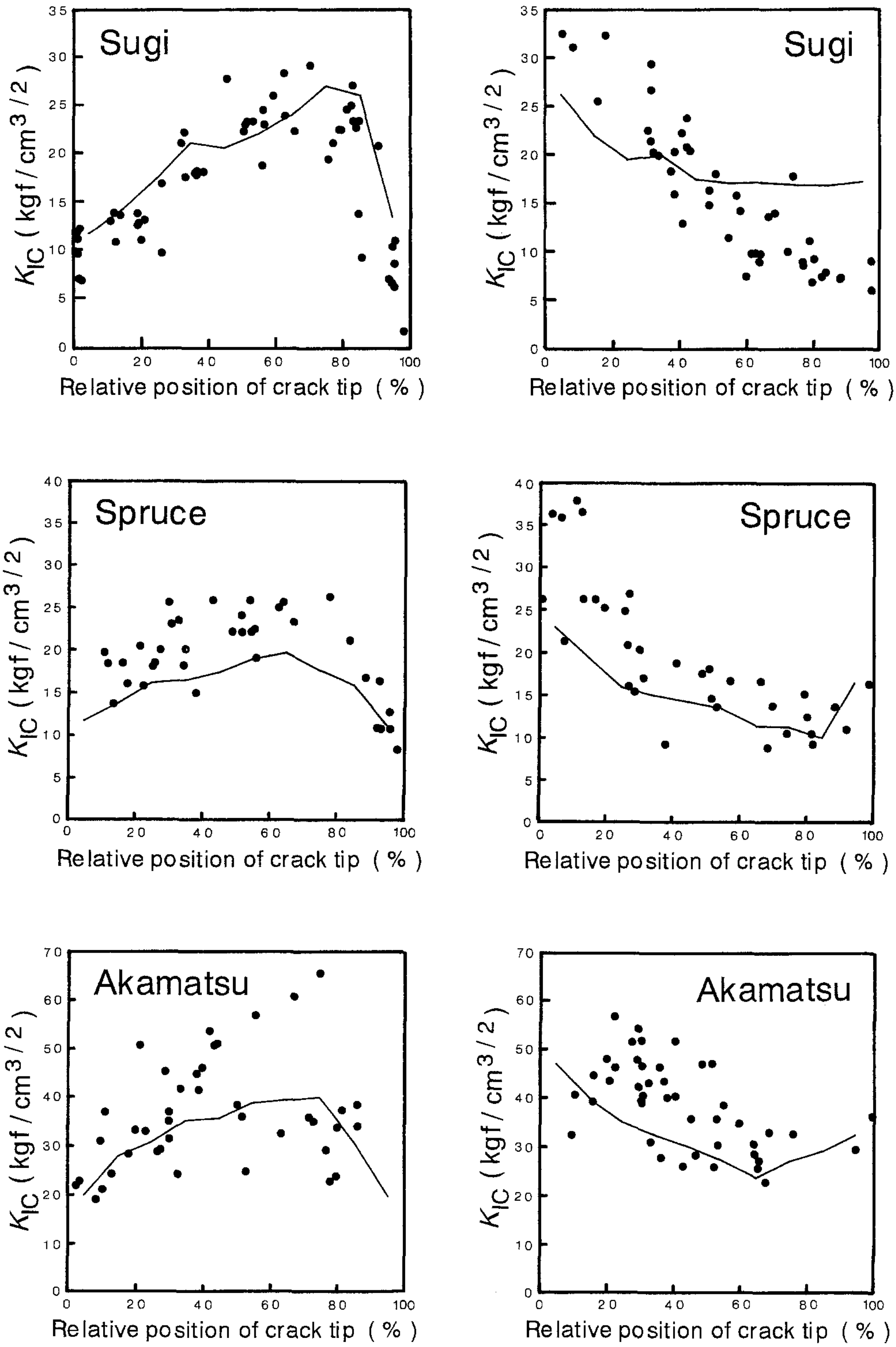


**Fig. 9.** Relations between the $K_{IC}$ value and the location of a crack tip in a single annual ring. **Left** Pith-side notched. **Right** Bark-side notched. *Circles*, $K_{IC}$ by experiment; *solid lines*, $K_{IC}$ by the finite element method

The results of measurements of acoustic emission (AE) and fractography of spruce in our previous report[2] were compared with the results from the present work and can be summarized as follows. When the degree of stress concentration was small, an AE of a small amplitude was gradually generated, and intrawall failure was clearly observed at the fracture surface that was considered to be formed before the crack initiation. On the other hand, when the degree of stress concentration was large, an AE of large amplitude was rapidly generated, and transwall failure was clearly observed. Considering the behavior before crack initiation, we believe that intrawall failure generated by a low level of concentration of stress relaxes stress concentration at the crack tip and contributes to the increased $K_{IC}$ value.

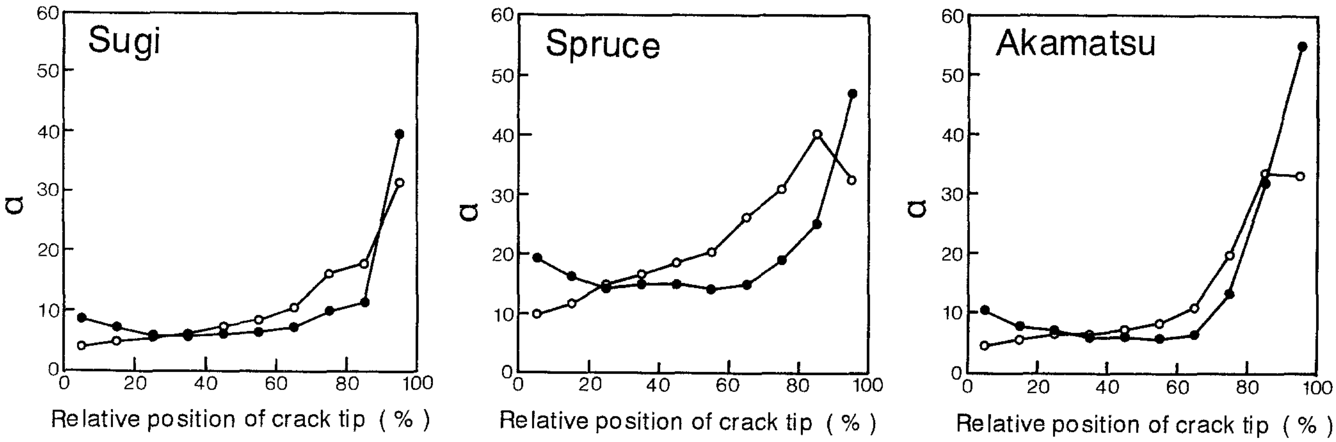


**Fig. 10.** Relations between the stress concentration factor ($\alpha$) and the location of a crack tip in a single annual ring. *Filled circles*, pith-side notched; *open circles*, bark-side notched

## Conclusions

The effects of the location of the crack tip in an annual ring and the direction of crack propagation on the fracture toughness of the TR crack propagation system of coniferous wood were analyzed by the finite element method in regard to changes in elastic modulus and strength within an annual ring. In terms of the variability of $K_{IC}$ values, the experimental and calculated results had the same tendency. Therefore, it was concluded that the variability of $K_{IC}$ is caused by (1) the heterogeneity of the elastic modulus and strength within an annual ring and (2) the changes in the degree of stress concentration at the crack tips, depending on the direction of crack propagation.

**Acknowledgments** We thank Dr. M. Fushitani and Dr. K. Sato of the Tokyo University of Agriculture and Technology for free use of testing machines and their helpful suggestions, and the late Mr. K. Tsuchiya for his cooperation in conducting our experiment.

## References

1. Ando K, Sato K, Fushitani M (1991) Fracture toughness and acoustic emission characteristics of wood. I. Effect of the location of a crack tip in an annual ring (in Japanese). Mokuzai Gakkaishi 37:1129–1134
2. Ando K, Ohta M (1995) Relationships between the morphology of micro-fractures of wood and the acoustic emission characteristics. Mokuzai Gakkaishi 41:640–646
3. Barrett JD, Foschi RO (1977) Mode II stress-intensity factors for cracked wood beams. Eng Frac Mech 9:371–378
4. Cramer SM, Goodman JR (1983) Model for stress analysis and strength prediction of lumber. Wood Fiber Sci 15:338–349
5. Triboulot P, Jodin P, Pluvinage G (1984) Validity of fracture mechanics concepts applied to wood by finite element calculation. Wood Sci Technol 18:51–58
6. Masuda M (1986) Theoretical consideration on fracture criteria of wood (in Japanese). Bull Kyoto Univ For 58:241–250
7. Zandbergs JG, Smith FW (1988) Finite element fracture prediction for wood with knots and cross grain. Wood Fiber Sci 20:97–106
8. Masuda M, Honda R (1994) Theoretical analysis on bending of lumber containing knots by using finite element method (in Japanese). Mokuzai Gakkaishi 40:127–133
9. Ohgama T, Masuda M, Yamada T (1977) Stress distribution within cell wall of wood subjected to tensile force in transverse direction (in Japanese). Zairyo 26:433–438
10. Ohgama T, Yamada T (1981) Young's moduli of earlywood and latewood in transverse direction of softwoods (in Japanese). Zairyo 30:707–711
11. Okamura H (1976) Introduction to linear fracture mechanics (in Japanese). Baihukan, Tokyo, p 217
12. Koshijima T, Sugihara H, Hamada R, Fukuyama M, Fuse G (1983) Light, friction, sound and vibration (in Japanese). In: Fundamental wood engineering. Bunkyo-Shuppan, Osaka, pp 93–104
13. Fushitani M, Kikata Y, Okano T, Sado T, Takemura T, Norimoto M, Arima T, Tsutsumi J, Hirai N (1985) Elasticity (in Japanese). In: Physics of wood. Bun-eido, Tokyo, pp 94–115
14. Fushitani M, Kikata Y, Okano T, Sado T, Takemura T, Norimoto M, Arima T, Tsutsumi J, Hirai N (1985) Strength (in Japanese). In: Physics of wood. Bun-eido, Tokyo, pp 140–167
15. Sawada M (1963) Elasticity and strength of wood as an orthotropic material (in Japanese). Zairyo 12:749–753